Cancer Cell Detection

DOI: 10.1002/anie.201203767

A Multicolor Nanoprobe for Detection and Imaging of Tumor-Related mRNAs in Living Cells**

*Na Li, Chenyang Chang, Wei Pan, and Bo Tang**

Cancer is a leading cause of death worldwide and accounts for several millions of deaths every year.[1] The survival of cancer patients is strongly associated with the stage of the tumor at the time of diagnosis. Identifying the cancer at the cellular level in an early stage before metastasis holds great promise for increasing the survival of cancer patients. A major focus of research towards this goal is on the estimation of abnormalities in gene expression in living cells.[2–4] Tumor-related mRNA has been widely used as a specific marker to assess the migration of tumor cells locally or in the bloodstream. Changes in the level of tumor-related mRNA expression are correlated with tumor burden and malignant progression.[5] The detection of tumor-related mRNA markers in intact cancer cells provides new tools for identifying cancer cells in clinical samples.

Recently, a variety of techniques have been exploited to monitor tumor-related mRNAs.[6] Among these methods, fluorescence imaging analysis offers an appealing approach for the detection of cancer at the cellular level, which may be of prognostic significance. Many fluorescence probes have been synthesized for the detection and imaging of mRNA in cancer cells and most of the research focuses on detecting a single type of mRNA,[4,7] which may yield false positive results and limits the development of intracellular mRNA imaging and detection. Notably, cancer is associated with multiple tumor-related mRNAs,[8] and some mRNA markers are expressed in normal cells.[9] Simultaneous detection of multiple targets brings new opportunities for improving the accuracy of early cancer detection over the single-marker assay. Although various types of platforms for the detection of multiple targets have been developed,[10] none have been designed for imaging three or more markers in living cells. Such intracellular imaging techniques for multiple tumor-related mRNAs could promote the progress of early cancer detection.

Herein, we describe a multicolor fluorescence nanoprobe based on nanoflares, which simultaneously detects three intracellular tumor-related mRNAs.[4] The nanoprobe consists of gold nanoparticles (Au NPs) functionalized with a dense shell of recognition sequences (synthetic oligonucleotides) hybridized to three short dye-terminated reporter sequences by gold–thiol bond formation (Figure 1).[11] The recognition sequences contain 21-base recognition elements for three specific mRNA transcripts: c-myc mRNA, TK1 mRNA, and GalNAc-T mRNA.

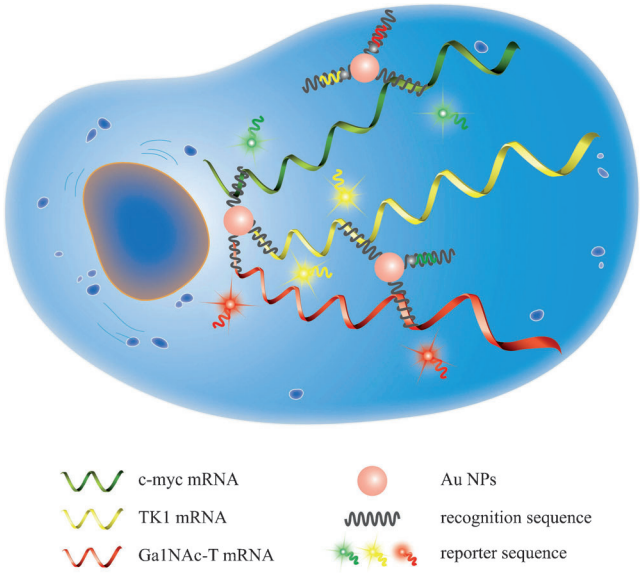

Figure 1. Illustration of the multicolor nanoprobe for the detection of intracellular tumor-related mRNAs.

Although they are important markers in cancer cells, these transcripts have rarely been previously imaged in living cells.[12–14] C-myc is a potent activator of tumorigenesis, and it is deregulated in a range of cancers. In particular, it plays a critical role in breast tumorigenesis and progression.[12] TK is an important
pyrimidine metabolic pathway enzyme, which includes two major isoenzymes (TK1 and TK2) and catalyzes the phosphorylation of thymidine to deoxythymidine monophosphate. TK1 is associated with cell division and is proposed to be a marker for tumor growth.[13] GalNAc-T is a key enzyme in the biosynthetic pathway of gangliosides GM2/GD2, which

[*] Dr. N. Li, C. Chang, W. Pan, Prof. B. Tang
College of Chemistry, Chemical Engineering and Materials Science
Engineering Research Center of Pesticide and Medicine Intermediate Clean Production, Ministry of Education
Key Laboratory of Molecular and Nano Probes, Ministry of Education
Shandong Normal University, Jinan 250014 (P.R. China)
E-mail: tangb@sdnu.edu.cn

[**] This work was supported by the National Key Natural Science Foundation of China (21035003), the National Natural Science Foundation of China (21105059), the Specialized Research Fund for the Doctoral Program of Higher Education of China (20113704130001), the Shandong Distinguished Middle-Aged and Young Scientist Encourage and Reward Foundation (BS2011L037), the Science and Technology Planning Project of Higher Education of Shandong Province, China (J10LB02), and the Program for Changjiang Scholars and Innovative Research Team in University.

Supporting information for this article is available on the WWW under http://dx.doi.org/10.1002/anie.201203767.

are elevated in expression on the surface of various types of cancer cells.[14] The reporter sequences are labeled by Rh110, Cy3, and Cy5 dyes, respectively (for details see the Supporting Information, Table S1). The fluorescence of the three dyes was quenched by Au NPs. In the presence of DNA or RNA targets, the recognition sequences hybridize with the complementary target sequences by forming the longer and more stable duplexes, causing the release of the reporter sequences, which can then produce fluorescence signals correlated with the relative amount of the specific DNA or RNA targets. The details of this approach are shown in Figure 1.

To the best of our knowledge, this is the first time that a nanoprobe has been used for imaging three targets in living cells. The nanoprobe takes advantage of the unique properties of Au NPs, such as great quenching efficiency,[15] great quenching distance[16] (which is beneficial for multicolor detection), resistance to degradation,[17] and the ability to enter cells without the use of transfection agents.[4] Moreover, it can effectively distinguish breast cancer cells from normal breast cells, as well as liver cancer cells from normal liver cells. Importantly, it can also identify the levels of mRNA expression, which would be beneficial for evaluation of the stage of tumor progression and in making treatment decisions. This novel approach could provide comprehensive and dependable information for early detection of cancer and avoid false positive results caused by detection of a single tumor-related mRNA.

We designed the nanoprobe using 13 nm Au NPs, because it has been reported that Au NPs of this size are efficient quenchers, can be densely functionalized with oligonucleotides,[18] and do not efficiently scatter visible light, which is important for designing optical probes with minimal interference.[4] The TEM images of Au NPs and nanoprobes (Au NPs functionalized with three flare duplexes) are shown in the Supporting Information, Figure S1. The results showed that the border of the Au NPs was clear and that of the nanoprobe was ambiguous, a result which is indicative of the assembly of flare duplexes on the surface of Au NPs. The UV/Vis absorption spectra indicated that the maximum absorption of the Au NPs was at 519 nm and that it was red-shifted to 524 nm for the nanoprobe, which further confirmed that the Au NPs were successfully functionalized with flare duplexes (Figure S2). Based on the previously established method,[19] each Au NP was calculated to carry 13 ± 1 Rh110-labeled flares targeting c-myc mRNA, 14 ± 1 Cy3-labeled flares targeting TK1 mRNA and 14 ± 1 Cy5-labeled flares targeting GalNAc-T mRNA. Details of the characterization are provided in Figure S3.

Binding studies were performed with the perfectly matched DNA targets for the three flare duplexes to evaluate the feasibility of the nanoprobe for the simultaneous detection of multiple DNA targets. For comparison, DNA targets with a single-base mismatch were also used under the same conditions. The results demonstrated that the probe responded with 5.9-fold, 4.4-fold, and 4.8-fold increases in fluorescence signals upon target recognition and binding for the Rh110-labeled duplex, Cy3-labeled duplex, and Cy5-labeled duplex, respectively. In contrast, the signals did not obviously change in the presence of single-base mismatched targets and were of comparable magnitude to the background fluorescence (Figure 2). These results indicated that the nanoprobe was efficient at signaling the presence of specific targets. Figure S4 shows that the fluorescence intensity of the nanoprobe increases with increasing concentration of the DNA targets from 0 to 200 nM, thus suggesting that the hybridization of the nanoprobe and DNA targets led to fluorescence recovery and that the fluorescence intensity is associated with the concentration of the DNA targets. The detection limit of the nanoprobe was calculated to be 1.2 nM for c-myc mRNA, 1.4 nM for TK1 mRNA, and 1.6 nM for GalNAc-T mRNA, respectively. The selectivity of flare duplexes for the nanoprobe is shown in Figure S5. The results revealed that every flare duplex was specifically bound to the respective DNA target and generated 4- to 6-fold higher fluorescent signal when mixed with the specific DNA target, as compared to other targets.

Nuclease stability is a key property of probes for diagnostic applications in living cells. A series of experiments was conducted using the enzyme deoxyribonuclease I (DNase I), a common endonuclease,[17] to evaluate the nuclease stability of the nanoprobe. The results showed that the nanoprobe treated with DNase I was not obviously degraded compared to the probe without DNase I (Figure 3). When the equivalent DNA targets were added to the nanoprobe-only and nanoprobe/DNase I solutions, respectively, the fluorescence intensity of the three dyes in both solutions was enhanced greatly after hybridization (Figure 3, insets). This indicates that the nanoprobe possesses

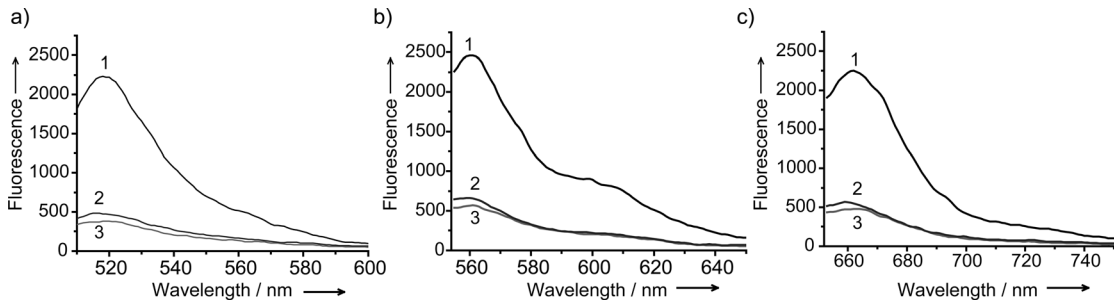

Figure 2. Multiplexing detection using the nanoprobe. The nanoprobe (1 nM, curve 3) was hybridized with three different perfectly matched targets (curve 1) and three different single-mismatched targets (curve 2); target concentrations are 200 nM. a) c-myc (Rh110, green emission at 520 nm). b) TK1 (Cy3, yellow emission at 560 nm). c) GalNAc-T (Cy5, red emission at 668 nm).

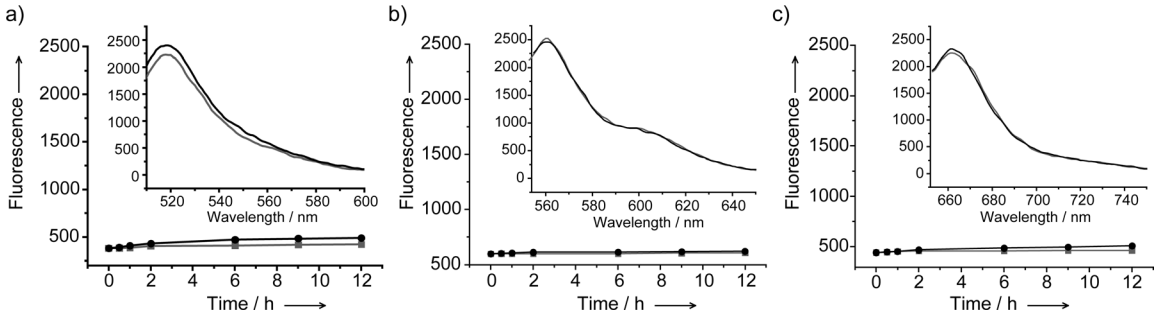

Figure 3. Nuclease stability of the nanoprobe in the presence or absence of DNase I. Fluorescence curves of the nanoprobe (1 nM) in buffer with (—●—) or without (—■—) DNase I, as a function of time. Insets: fluorescence spectra after hybridization of the nanoprobe with DNA targets in the presence (——) and absence (——) of DNase I. a) C-myc target measured with excitation at 490 nm. b) TK1 target measured with excitation at 550 nm. c) GalNAc-T target measured with excitation at 648 nm.

high resistance to nuclease, and further confirmed that the fluorescence recovery was indeed due to the hybridization of the nanoprobe and targets instead of nuclease degradation.

To evaluate the cytotoxicity of the nanoprobe, we performed an MTT (3-(4,5-dimethylthiazol-2-yl)-2,5-diphenyltetrazolium bromide) assay in human breast cancer cell line MCF-7 as an example. The absorbance of MTT at 490 nm is dependent upon the degree of activation of the cells. The cell viability is then expressed by the ratio of the absorbance of the cells incubated with the nanoprobe to that of the cells incubated with the culture medium only. The results indicated that the unmodified Au NPs (1 nM) and the nanoprobe (1 nM and 5 nM) showed almost no cytotoxicity or side effects in living cells (Figure S6), and confirmed that the nanoprobe could be used in intracellular marker diagnosis.

For the application of the nanoprobe in detecting multiple mRNAs simultaneously, in vitro binding and uptake studies were performed with MCF-7 and the normal immortalized human mammary epithelial cell line MCF-10A, where c-myc, TK1, and GalNAc-T transcripts were all overexpressed.[12–14] As can be seen from Figure 4, after MCF-7 was incubated with the nanoprobe, a strong green fluorescence signal for c-myc mRNA, a yellow fluorescence signal for TK1 mRNA, and a red fluorescence signal for GalNAc-T mRNA were observed under confocal laser scanning microscopy (CLSM). When MCF-10A cells were incubated with the nanoprobe under the same conditions, all of the three fluorescence signals were very low, indicating that the nanoprobe can be used as a fluorescence probe for the detection of breast cancer. To confirm the uptake of the nanoprobe in MCF-10A, an approach based on inductively coupled plasma atomic emission spectroscopy (ICP-AES) was employed.[20] The analysis showed that the nanoprobe was taken up in MCF-10A cells(see the Supporting Information). Bright-field images confirmed that the cells were viable throughout the imaging experiments. Moreover, the three fluorescence signals are well overlapped in the cytoplasm, indicating that the nanoprobe mostly accumulated in the cytoplasm and can simultaneously detect multiple gene expression in a single cell. Reverse transcription-PCR (RT-PCR) also showed that the relative expression levels of the three tumor-related mRNAs in MCF-7 were higher than in MCF-10A (Figure S7a). Next, we applied the nanoprobe to the simultaneous detection of multiple mRNAs in human hepatocellular liver carcinoma cell line HepG2 and human hepatocyte cell line HL-7702. Strong green, yellow, and red fluorescence signals for the three mRNAs were also observed under CLSM in HepG2 after incubation with the nanoprobe, which was similar to the results obtained with MCF-7. Interestingly, after HL-7702 was incubated with the nanoprobe, the green and yellow fluorescence signals were faint, while the red fluorescent signal was strong, indicating that the expression of GalNAc-T mRNA in HL-7702 was also high. The RT-PCR results further verified that the relative levels of c-myc and TK1 mRNA in HepG2 were higher than in HL-7702, while the levels of GalNAc-T mRNA were similar in HL-7702 and HepG2, indicating that the expression levels of GalNAc-T mRNA in HL-7702 and HepG2 were both high (Figure S7b). These results show that the fluorescent signals produced by the multicolor nanoprobe were consistent with the levels of tumor-related mRNA gene expression, and suggest that the detection of multiple tumor-related mRNAs could avoid the false positive results yielded by testing for single tumor-related mRNAs. Moreover, the above results revealed that the nanoprobe could be used for the discrimination of cancer cells from normal cells.

The relative expression levels of tumor-related mRNAs in cancer cells are different in the various stages of tumor progression, and it is critical to evaluate their relative expression levels for estimating the tumor stage and making treatment decisions. We next investigated the ability of the nanoprobe to detect the changes in the mRNA expression levels in living cells. TK1 mRNA in MCF-7 was chosen as an example. It was reported that tamoxifen induced the down-regulation of TK1 mRNA expression and β-estradiol induced the up-regulation of TK1 mRNA expression.[21] MCF-7 cells were divided into three groups. One group was treated with tamoxifen to decrease the TK1 mRNA expression and another one was treated with β-estradiol to increase the TK1 mRNA expression. An untreated group served as a control. The nanoprobe was then incubated with the treated and untreated cells. The fluorescence intensity was lower in the tamoxifen treated MCF-7 cells (Figure S8b) and higher in the β-estradiol treated MCF-7 cells (Figure S8c), relative to that in the untreated cells (Figure S8a). The bright-field images (Figure S8d,e,f) showed that the cells were viable

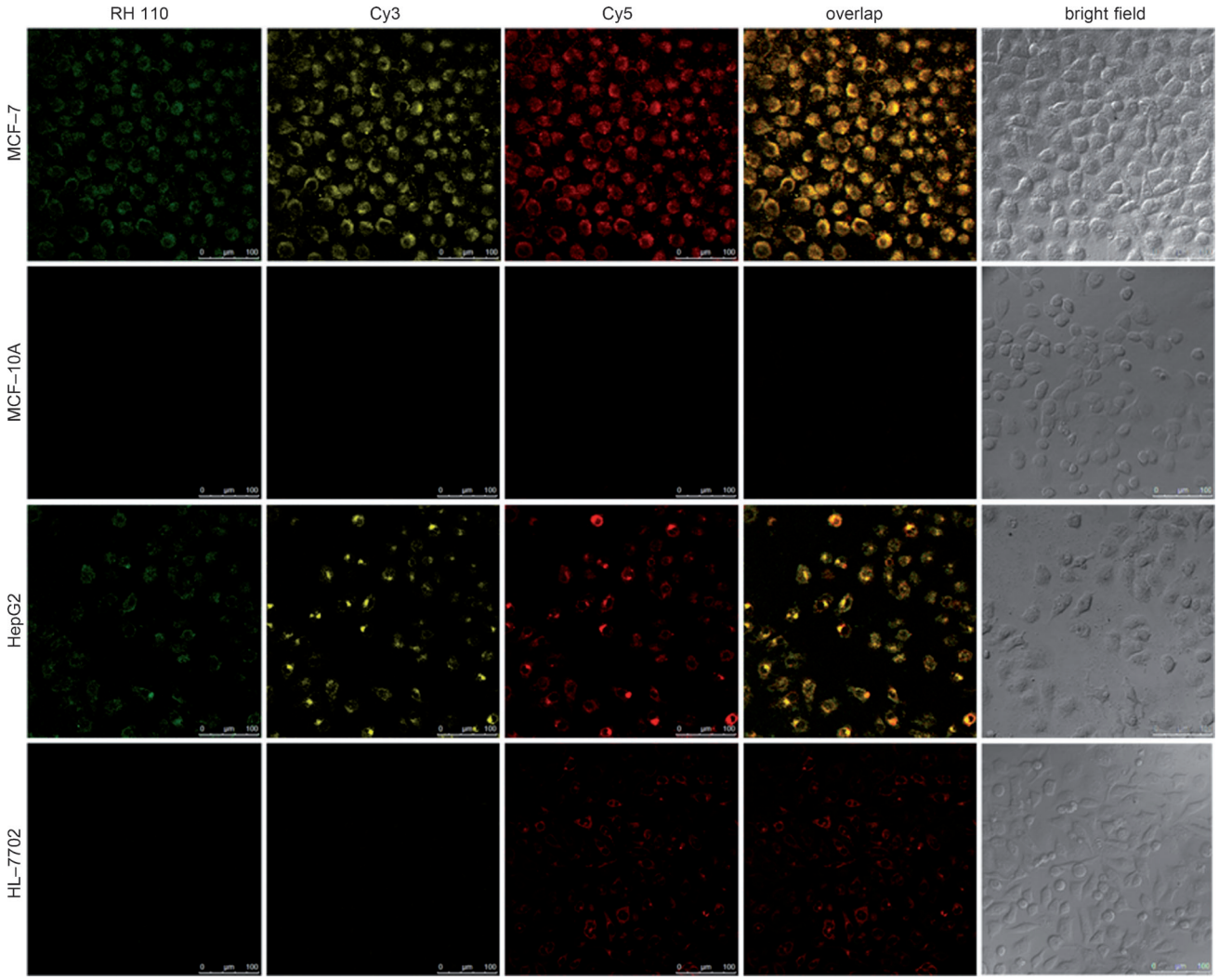

Figure 4. Intracellular imaging of c-myc mRNA, TK1 mRNA, and GalNAc-T mRNA under CLSM. MCF-7, MCF-10A, HepG2, and HL-7702 cells were incubated with the nanoprobe (1 nM) for 12 h at 37 °C. The c-myc mRNA was recorded using Rh110 in the green channel with excitation at 488 nm ; TK1 mRNA was recorded using Cy3 in the yellow channel with excitation at 543 nm; GalNAc-T mRNA was recorded using Cy5 in the red channel with excitation at 633 nm. Scale bars are 100 μm.

throughout the imaging experiment. RT-PCR further confirmed that the level of TK1 mRNA expression decreased after tamoxifen treatment and increased after β-estradiol treatment (Figure S9). These results indicate that the fluorescence intensity correlates well with the level of tumor-related mRNA expression in living cells. Thus, the nanoprobe is capable of detecting changes in gene expression levels in cancer cells.

In summary, we have presented a novel nanoprobe, based on multicolor nanoflares, that can simultaneously detect and image three types of tumor-related mRNAs in living cells. The nanoprobe exhibits high specificity, nuclease stability and good biocompatibility. Moreover, the nanoprobe could effectively distinguish cancer cells from normal cells and identify changes in the expression levels of tumor-related mRNAs in living cells, which would be beneficial in evaluating the stage of tumor progression and in making treatment decisions. Compared to the traditional detection of single tumor-related mRNAs, the current approach could offer more comprehensive and reliable information for cancer detection, and effectively prevent false positive results. We anticipate that the nanoprobe will provide new opportunities for detection and imaging of multiple markers in living cells.

Received: May 16, 2012
Published online: July 2, 2012

Keywords: gold · mRNA · multicolor nanoprobes · nanoparticles · cancer detection

[1] a) World Health Organization. The Global Burden of Disease: 2004 Update. Geneva: World Health Organization, **2008**; b) A. Jemal, F. Bray, M. M. Center, J. Ferlay, E. Ward, D. Forman, *Ca-Cancer J. Clin.* **2011**, *61*, 69 – 90; c) B. Taback, A. D. Chan, C. T. Kuo, P. J. Bostick, H. J. Wang, A. E. Giuliano, D. S. B. Hoon, *Cancer Res.* **2001**, *61*, 8845 – 8850.

[2] a) D. Hanahan, R. A. Weinberg, *Cell* **2000**, *100*, 57 – 70; b) K. L. Nathanson, R. Wooster, B. L. Weber, K. N. Nathanson, *Nat.*

Med. **2001**, *7*, 552 – 556; c) X. H. Peng, Z. H. Cao, J. T. Xia, G. W. Carlson, M. M. Lewis, W. C. Wood, L. Yang, *Cancer Res.* **2005**, *65*, 1909 – 1917.
[3] P. J. Santangelo, B. Nix, A. Tsourkas, G. Bao, *Nucleic Acids Res.* **2004**, *32*, e57.
[4] D. S. Seferos, D. A. Giljohann, H. D. Hill, A. E. Prigodich, C. A. Mirkin, *J. Am. Chem. Soc.* **2007**, *129*, 15477 – 15479.
[5] H. Schwarzenbach, D. S. B. Hoon, K. Pantel, *Nat. Rev. Cancer* **2011**, *11*, 426 – 437.
[6] a) T. Nolan, R. E. Hands, S. A. Bustin, *Nat. Protoc.* **2006**, *1*, 1559 – 1582; b) J. Couzin, *Science* **2006**, *313*, 1559 – 1559; c) A. E. Prigodich, D. S. Seferos, M. D. Massich, D. A. Giljohann, B. C. Lane, C. A. Mirkin, *ACS Nano* **2009**, *3*, 2147 – 2152.
[7] a) Y. Gao, G. M. Qiao, L. H. Zhuo, N. Li, Y. Liu, B. Tang, *Chem. Commun.* **2011**, *47*, 5316 – 5318; b) G. M. Qiao, L. H. Zhuo, Y. Gao, L. J. Yu, N. Li, B. Tang, *Chem. Commun.* **2011**, *47*, 7458 – 7460; c) Y. Kam, A. Rubinstein, A. Nissan, D. Halle, E. Yavin, *Mol. Pharmaceutics* **2012**, *9*, 685 – 693.
[8] D. Sidransky, *Science* **1997**, *278*, 1054 – 1058.
[9] R. Jung, K. Peterson, W. Kruger, M. Wolf, C. Wagener, A. Zander, *Br. J. Cancer* **1999**, *81*, 870 – 873.
[10] a) S. Tyagi, D. P. Bratu, F. R. Cramer, *Nat. Biotechnol.* **1998**, *16*, 49 – 53; b) S. J. He, B. Song, D. Li, C. F. Zhu, W. P. Qi, Y. Q. Wen, L. H. Wang, S. P. Song, H. P. Fang, C. H. Fan, *Adv. Funct. Mater.* **2010**, *20*, 453 – 459; c) G. M. Qiao, Y. Gao, N. Li, Z. Z. Yu, L. H. Zhuo, B. Tang, *Chem. Eur. J.* **2011**, *17*, 11210 – 11215; d) S. P. Song, Z. Q. Liang, J. Zhang, L. H. Wang, G. X. Li, C. H. Fan, *Angew. Chem.* **2009**, *121*, 8826 – 8830; *Angew. Chem. Int. Ed.* **2009**, *48*, 8670 – 8674; e) Y. Huang, S. L. Zhao, H. Liang, Z. F. Chen, Y. M. Liu, *Chem. Eur. J.* **2011**, *17*, 7313 – 7319.
[11] a) C. A. Mirkin, R. L. Letsinger, R. C. Mucic, J. J. Storhoff, *Nature* **1996**, *382*, 607 – 609; b) R. Elghanian, J. J. Storhoff, R. C. Mucic, R. L. Letsinger, C. A. Mirkin, *Science* **1997**, *277*, 1078 – 1081; c) S. J. Park, T. A. Taton, C. A. Mirkin, *Science* **2002**, *295*, 1503 – 1506.
[12] a) N. Meyer, L. Z. Penn, *Nat. Rev. Cancer* **2008**, *8*, 976 – 990; b) D. J. Liao, R. B. Dickson, *Endocr.-Relat. Cancer* **2000**, *7*, 143 – 164; c) J. H. Xu, Y. H. Chen, O. I. Olopade, *Genes Cancer* **2010**, *1*, 629 – 640; d) A. Efstratiadis, M. Szabolcs, A. Klinakis, *Cell Cycle* **2007**, *6*, 418 – 429.
[13] a) C. C. Chen, T. W. Chang, F. M. Chen, M. F. Hou, S. Y. Hung, I. W. Chong, S. C. Lee, T. H. Zhou, S. R. Lin, *Oncology* **2006**, *70*, 438 – 446; b) J. F. R. Robertson, K. L. O'Neill, M. W. Thomas, P. G. McKenna, R. W. Blamey, *Br. J. Cancer* **1990**, *62*, 663 – 667; c) P. Broet, S. Romain, A. Daver, G. Ricolleau, V. Quillien, A. Rallet, B. Asselain, P. M. Martin, F. Spyratos, *J. Clin. Oncol.* **2001**, *19*, 2778 – 2787.
[14] a) B. Taback, A. D. Chan, C. T. Kuo, P. J. Bostick, H. J. Wang, A. E. Giuliano, D. S. B. Hoon, *Cancer Res.* **2001**, *61*, 8845 – 8850; b) C. T. Kuo, P. J. Bostick, R. F. Irie, *Clin. Cancer Res.* **1998**, *4*, 411 – 418; c) T. Tai, J. C. Paulson, L. D. Cahan, R. F. Irie, *Proc. Natl. Acad. Sci. USA* **1983**, *80*, 5392 – 5396; d) D. S. Hoon, M. Banez, E. Okun, D. L. Morton, R. F. Irie, *Cancer Res.* **1991**, *51*, 2002 – 2008.
[15] B. Dubertret, M. Calame, A. J. Libchaber, *Nat. Biotechnol.* **2001**, *19*, 365 – 370.
[16] E. Dulkeith, M. Ringler, T. A. Klar, J. Feldmann, A. M. Javier, W. J. Parak, *Nano Lett.* **2005**, *5*, 585 – 589.
[17] D. S. Seferos, A. E. Prigodich, D. A. Giljohann, P. C. Patel, C. A. Mirkin, *Nano Lett.* **2009**, *9*, 308 – 311.
[18] A. P. Alivisatos, K. P. Johnsson, X. Peng, T. E. Wilson, C. J. Loweth, M. P. Bruchez, P. G. Schultz, *Nature* **1996**, *382*, 609 – 611.
[19] L. M. Demers, C. A. Mirkin, R. C. Mucic, R. A. Reynolds, R. L. Letsinger, R. Elghanian, G. Viswanadham, *Anal. Chem.* **2000**, *72*, 5535 – 5541.
[20] a) B. D. Chithrani, A. A. Ghazani, W. C. W. Chan, *Nano Lett.* **2006**, *6*, 662 – 668; b) S. A. Love, C. L. Haynes, *Anal. Bioanal. Chem.* **2010**, *398*, 677 – 688; c) C. Freese, M. I. Gibson, H. A. Klok, R. E. Unger, C. J. Kirkpatrick, *Biomacromolecules* **2012**, *13*, 1533 – 1543.
[21] a) A. Kasid, N. E. Davidson, E. P. Gelmann, M. E. Lippman, *J. Biol. Chem.* **1986**, *261*, 5562 – 5567; b) J. A. Foekens, S. Romain, M. P. Look, P. M. Martin, J. G. M. Klijn, *Cancer Res.* **2001**, *61*, 1421 – 1425.

